

# Hierarchical Nanoparticle/Block Copolymer Surface Features via Synergistic Self-Assembly at the Air–Water Interface

Robert B. Cheyne and Matthew G. Moffitt\*

Department of Chemistry, University of Victoria, P.O. Box 3065,  
Victoria, BC, V8W 3V6, Canada

Received July 18, 2005. In Final Form: September 20, 2005

This work demonstrates the first example of the controlled organization of semiconducting nanoparticles (NPs) using amphiphilic block copolymer self-assembly at the air–water interface. Preferential interactions between polystyrene-functionalized NPs and the polystyrene block of an amphiphilic polystyrene-*b*-poly(ethylene oxide) block copolymer result in synergistic self-assembly at the air–water interface, forming a range of highly stable one-dimensional NP/polymer surface features, including branched nanowires, nanocables up to 100  $\mu\text{m}$  in length, and nanowires with nanoring connectors. This strategy offers new routes to hierarchical hybrid assemblies with potential photonics applications because the nanoscale organization of NPs is coupled to features with dimensions that are commensurate with optical wavelengths.

In this letter, we present the first example of the controlled organization of semiconducting nanoparticles (NPs) using amphiphilic block copolymer self-assembly at the air–water interface. The controlled assembly of metal and semiconducting NPs into one-dimensional (1D) and two-dimensional (2D) superstructures is a critical step toward their use as functional elements in new materials because collective properties and function are governed by NP organization on a combination of length scales.<sup>1–13</sup> Self-assembly strategies that combine the control of NP organization with the incorporation of NPs into a polymeric matrix offer additional possibilities for tuning the mechanical, optical, electronic, magnetic, and catalytic properties of new nanostructured composites. Block copolymers have recently been shown to provide a molecular handle on this challenge by promoting NP organization within a wide range of patterns arising from microphase separation.<sup>10–13</sup> To date, the vast majority of work employing block copolymers to direct NP assembly has involved block copolymers in the solid state, in which domain patterns are highly periodic and feature sizes are on the order of tens of nanometers. However, for many future applications, the need to couple nanometer-scale NP organization with meso- and micron-scale features (e.g., commensurate

with optical wavelengths) is critical. Additionally, polymer self-assembly strategies resulting in controllable but nonperiodic structures could lead to functionally interesting hierarchical architectures that are inaccessible in more highly ordered systems.

The 2D self-assembly of amphiphilic block copolymers at the air–water interface is a proven route to patterned surfaces, which is in many ways distinct from block copolymer self-assembly in the bulk or in solution.<sup>14,15</sup> For example, the interfacial self-assembly of polystyrene-*b*-poly(ethylene oxide) (PS-*b*-PEO) has been demonstrated by depositing solutions of the copolymer in chloroform (a good solvent for both blocks) onto the surface of water, followed by evaporation of the solvent.<sup>16–18</sup> The formation of various 2D and 1D PS-*b*-PEO surface features by this method is the result of spontaneous copolymer aggregation at the air–water interface, which arises from an interplay of attractive interactions between the epiphilic PEO and the water surface and repulsive interactions between PS and water and PS and PEO as the chloroform evaporates; kinetic factors such as chain entanglements and the ultimate “freezing” of the glassy polymer can also influence the final morphologies.<sup>16,17</sup> Unlike block copolymer self-assembly in the bulk or in solution, the lateral dimensions of the aggregates obtained at the air–water interface can be orders of magnitude larger than the polymer chain dimensions,<sup>16–18</sup> suggesting that a large number of diblocks can overlap to form the surface features with block junctions localized underneath the aggregates. The interfacial self-assembly of block copolymers is therefore a potentially exciting route toward novel structures with lateral features ranging from the meso- to micron-scale. In addition, monolayers of polymeric surface features obtained by self-assembly at the air–water interface can be easily transferred by the Langmuir–Blodgett (LB) method to various solid substrates for potential applica-

- (1) Tang, Z.; Kotov, N. A. *Adv. Mater.* **2005**, *17*, 951.
- (2) Sear, R. P.; Chung, S.-W.; Markovich, G.; Gelbart, W. M.; Heath, J. R. *Phys. Rev. E* **1999**, *59*, 6255.
- (3) Hassenkam, T.; Nørgaard, K.; Iversen, L.; Kiely, C. J.; Brust, M.; Bjørnholm, T. *Adv. Mater.* **2002**, *14*, 1126.
- (4) Reuter, T.; Vidoni, O.; Torma, V.; Schmid, G.; Nan, L.; Gleiche, M.; Chi, L.; Fuchs, H. *Nano Lett.* **2002**, *2*, 709.
- (5) Fahmi, A. W.; Oertel, U.; Steinert, V.; Froeck, C.; Stamm, M. *Macromol. Rapid Commun.* **2003**, *24*, 625.
- (6) Rabani, E.; Reichman, D. R.; Geissler, P. L.; Brus, L. E. *Nature* **2003**, *426*, 271.
- (7) Maillard, M.; Motte, L.; Ngo, A. T.; Pileni, M. P. *J. Phys. Chem. B* **2000**, *104*, 11871.
- (8) Shah, P. S.; Sigman, M. B., Jr.; Stowell, C. A.; Lim, K. T.; Johnston, K. P.; Korgel, B. A. *Adv. Mater.* **2003**, *15*, 971.
- (9) Zhang, L.; Gaponik, N.; Müller, J.; Plate, U.; Weller, H.; Erker, G.; Fuchs, H.; Rogach, A. L.; Chi, L. *Small* **2005**, *1*, 524.
- (10) Lin, Y.; Böker, A.; He, J.; Sill, K.; Xiang, H.; Abetz, C.; Li, X.; Wang, J.; Emrick, T.; Long, S.; Wang, Q.; Balazs, A.; Russell, T. P. *Nature* **2005**, *434*, 55.
- (11) Chiu, J. J.; Kim, B. J.; Kramer, E. J.; Pine, D. J. *J. Am. Chem. Soc.* **2005**, *127*, 5036.
- (12) Bockstaller, M. R.; Lapetnikov, Y.; Margel, S.; Thomas, E. L. *J. Am. Chem. Soc.* **2003**, *125*, 5276.
- (13) Lopes, W. A.; Jaeger, H. M. *Nature* **2001**, *414*, 735.

- (14) Zhu, J.; Eisenberg, A.; Lennox, R. B. *J. Am. Chem. Soc.* **1991**, *113*, 5583.
- (15) Cox, J.; Eisenberg, A.; Lennox, R. B. *Curr. Opin. Colloid Interface Sci.* **1999**, *4*, 52.
- (16) Cheyne, R. B.; Moffitt, M. M. *Langmuir* **2005**, *21*, 5453.
- (17) Devereaux, C. A.; Baker, S. M. *Macromolecules* **2002**, *35*, 1921.
- (18) Cox, J. K.; Yu, K.; Constantine, B.; Eisenberg, A.; Lennox, R. B. *Langmuir* **1999**, *15*, 7714.

**Scheme 1. Cooperative Self-Assembly of PS–CdS and PS-*b*-PEO at the Air–Water Interface.**


tions, with the transfer surface pressure ( $\pi$ ) providing control of the distances between self-assembled aggregates.<sup>17</sup>

Here, we combine interfacial PS-*b*-PEO self-assembly with preferential interactions between PS brush-coated cadmium sulfide (PS–CdS) NPs and the PS block of PS-*b*-PEO, with the aim of directing NP organization at the air–water interface (Scheme 1). The PS–CdS “building blocks” are polystyrene-*b*-poly(cadmium acrylate) (PS-*b*-PACd)-stabilized CdS NPs (Scheme 1), which have been previously described.<sup>19–22</sup> The high- $T_g$  PACd layer of PS–CdS provides kinetic stability for the outer brush layer of PS chains ( $\sim 120$  repeat units), which gives the CdS NPs (average diameter = 3.6 nm) compatibility with various organic solvents and polymer media. Two different PS-*b*-PEO copolymer samples (Polymer Source) were employed to direct the interfacial self-assembly of PS–CdS: PS-*b*-PEO1 has a PS block length ( $N_{PS}$ ) of 1200 repeat units and a PEO block length ( $N_{PEO}$ ) of 370 units (11.4 wt % PEO), whereas PS-*b*-PEO2 is somewhat more hydrophilic, with  $N_{PS}$  = 1440 units and  $N_{PEO}$  = 800 units (18.9 wt % PEO).

Chloroform solutions of PS–CdS blended with either PS-*b*-PEO1 or PS-*b*-PEO2 in various proportions and to various concentrations were deposited dropwise at the air–water interface of a Langmuir trough (KSV 3000). Both the PS–CdS and PS-*b*-PEO components were well dispersed in chloroform, and no micellization of PS-*b*-PEO was detected in the spreading solutions by light scattering; however, the evaporation of chloroform at the surface of water induced the self-assembly of PS–CdS and PS-*b*-PEO. The resulting features were then compressed to the desired surface pressure ( $\pi$ ) and transferred vertically to glass substrates and transmission electron microscopy (TEM) grids, using the LB technique, for analysis with atomic force microscopy (AFM) and TEM.

Without added PS–CdS, the interfacial self-assembly of pure PS-*b*-PEO1 deposited from chloroform solutions of 1.0 or 2.0 mg/mL yielded a combination of dots and long spaghetti aggregates, with mean feature heights of 12–16 nm and mean widths of 160–170 nm (Figure 1a); under the same conditions, PS-*b*-PEO2 formed similar aggregates. Conversely, when pure PS–CdS was deposited from chloroform at the air–water interface without blending with either amphiphilic PS-*b*-PEO copolymer, the result was a very polydisperse population of circular islands with diameters between  $\sim 0.1$  to  $2 \mu\text{m}$  and heights up to 100 nm (Figure 1b); these polydisperse, circular aggregates are attributed to the hydrophobic, “PS-like” nature of PS–CdS, which will tend to minimize unfavorable contacts with the water surface.

Interestingly, the interfacial self-assembly of the blended components yielded various hybrid 1D features that were entirely different from the aggregates obtained from either

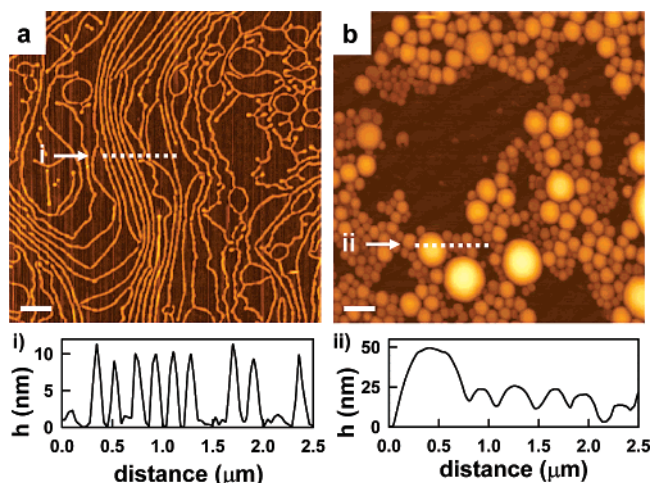


**Figure 1.** AFM images of (a) pure PS-*b*-PEO1 and (b) pure PS–CdS NPs, each deposited from 1.0 mg/mL chloroform solutions onto the air–water interface and then transferred to glass substrates via the LB technique; scale bars represent 1  $\mu\text{m}$ . Below each AFM image, a representative linear topological profile of the self-assembled aggregates is shown.

pure PS-*b*-PEO (Figure 1a) or pure PS–CdS (Figure 1b). The formation of these unique features suggests a synergistic, spontaneous organization of the amphiphilic copolymer and hydrophobic PS–CdS at the air–water interface, with the self-assembly of each component being coupled to simultaneous PS–PS attractive interactions between the components as chloroform evaporation occurs. AFM and TEM images of representative structures from 1:3 blends of PS-*b*-PEO1 and PS–CdS (PS–CdS weight fraction,  $f = 0.75$ ) at different spreading solution concentrations are shown in Figure 2. Unlike PS–CdS alone, these blends formed 1D (lateral aspect ratios  $\gg 1$ ) and pseudo-1D assemblies, including branched nanowires (Figure 2a,c) and extremely long aggregates, which we termed “nanocables” (Figure 2b,d). The widths ( $w$ ) of the nanowires and nanocables ( $w = 300 \pm 50$  nm) are quite uniform for structures of various lengths, although the feature lengths are polydisperse, ranging from 2 to  $20 \mu\text{m}$  for branched nanowires and up to  $100 \mu\text{m}$  for nanocables. We note that the widths of nanowires and nanocables from the self-assembly of PS–CdS/PS-*b*-PEO blends are  $\sim 2$  times greater than the widths of the spaghetti aggregates formed from PS-*b*-PEO alone, suggesting an incorporation of PS–CdS into the polymer features. In addition, the mean height ( $h$ ) of the 1D assemblies in Figure 2 is  $21 \pm 2$  nm, as determined by AFM topology profiles (Figure 2, profiles i and ii), which is higher than that of pure PS-*b*-PEO1 spaghetti aggregates ( $\sim 12$  nm; Figure 1a, profile i) and slightly less than the hydrodynamic diameter of PS–CdS measured by dynamic light scattering in chloroform (27 nm); the assemblies are also significantly shorter than the polydisperse islands obtained from pure PS–CdS (Figure 1b;  $h$  up to 100 nm). These data are consistent with a monolayer of PS–CdS NPs stabilized at the air–water interface within a laterally patterned PS-*b*-PEO brush structure (Scheme 1), compared to the multilayer islands obtained without added PS-*b*-PEO.

Confirmation of NP organization within the polymeric surface features was provided by TEM (Figure 2c,d), which allowed the internal distribution of dense CdS NPs to be imaged. Because different substrates were required for AFM and TEM, the exact same aggregates could not be imaged by both techniques; however, we were able to simultaneously transfer aggregates from a single mono-

(19) Moffitt, M.; McMahon, L.; Pessel, V.; Eisenberg, A. *Chem. Mater.* **1995**, *7*, 1185.

(20) Moffitt, M.; Vali, H.; Eisenberg, A. *Chem. Mater.* **1998**, *10*, 1021.

(21) Wang, C.-W.; Moffitt, M. G. *Langmuir* **2004**, *20*, 11784.

(22) Wang, C.-W.; Moffitt, M. *Chem. Mater.* **2005**, *17*, 3871.



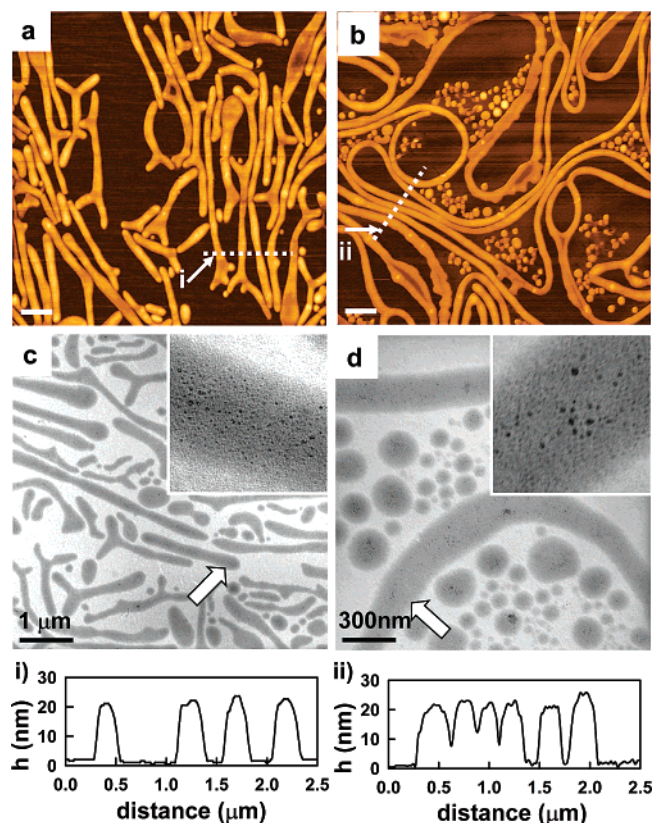


**Figure 2.** AFM (a,b) and TEM (c,d) images of representative hierarchical assemblies from blends of PS-CdS and PS-*b*-PEO1 deposited from chloroform onto the air-water interface. Spreading solution concentrations and PS-CdS weight fractions of the blends,  $f$ , were (a,c) 2.0 mg/mL,  $f = 0.75$  and (b,d) 1.0 mg/mL,  $f = 0.75$ , respectively. Film transfer occurred at 2.0 mN/m. The scale bars for the AFM images represent 1  $\mu$ m, and the scale bars for the TEM images are as indicated. Insets are magnified versions of the indicated regions of the TEM images (arrows) with edge lengths of 500 nm.

layer onto both substrate types using a modified LB dipper. Because the aggregates are kinetically frozen at the water surface following solvent evaporation, the nature of the substrate does not affect the observed structures; therefore, the dimensions and morphologies of the features observed by AFM and TEM were consistently similar for a given monolayer. Importantly, the TEM images clearly showed CdS NPs uniformly dispersed along the branched nanowires and nanocables, with average interparticle spacings of  $\sim 10$  nm. The lateral packing of NPs within the 1D superstructures was quite dense:  $\sim 10^3$  NPs for each micron length of nanowire or nanocable. We note that these NP/polymer features exhibit unique structural hierarchy, with NP organization on a combination of vastly disparate length scales via a single self-assembly step (Scheme 1). Compared to block copolymer-directed NP self-assembly in the bulk, in which the localization of block junctions at the domain interfaces limits characteristic feature sizes to polymer chain dimensions, the current strategy of interfacial self-assembly allows access to NP/polymer features with dimensions that are orders of magnitude larger than a polymer chain; this is attributed to the fact that the block junctions are localized at the air-water interface, such that features arise from the lateral organization of many chains arranged in a brush-like manner.

Because a uniform and monodisperse population of aggregates was not obtained in any of the monolayers investigated, no long-range order between features was

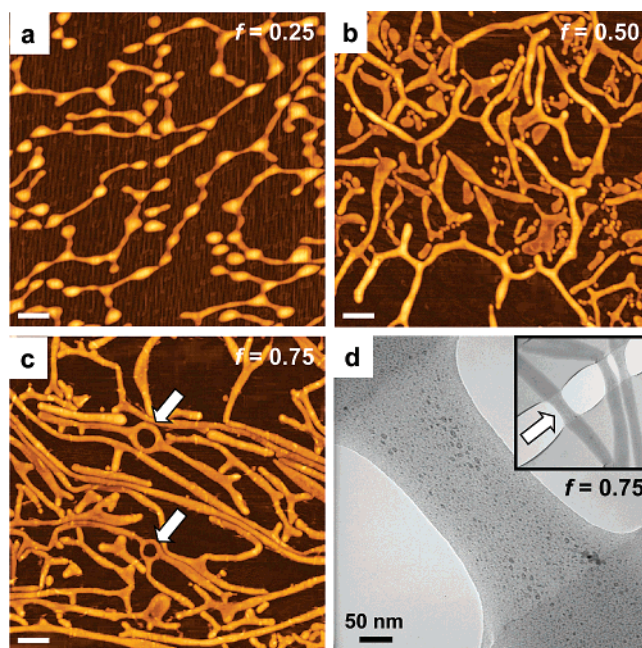


**Figure 3.** Representative AFM images (a-c) of PS-CdS/PS-*b*-PEO2 blends self-assembled at the air-water interface with different weight fractions of PS-CdS in the blends,  $f$ . Spreading solution concentrations were 2.0 mg/mL, and film transfer occurred at 5.0 mN/m in all cases;  $f$  for each image is described in the figure. The scale bars in the AFM images represent 1  $\mu$ m, and the arrows highlight features described in the text. The TEM image (d) shows nanowire aggregates subjected to a tensile stress from the torn Formvar substrate.

observed; however, some local ordering was apparent, with the shorter branched nanowires tending to orient in a single preferred direction on the substrate (Figure 2a). The origin of these spatial correlations between aggregates is believed to be compression on the surface of the Langmuir trough, which occurs once the individual aggregate morphologies have assembled and become kinetically "frozen" by solvent evaporation; this suggests potential for manipulating the order and density of hybrid aggregates on surfaces via self-assembly at the air-water interface.

By varying the composition of deposited PS-CdS/PS-*b*-PEO blends for a given spreading solution concentration, we were able to tune the morphologies of the resulting NP/polymer assemblies. Figure 3a-c shows AFM images of surface features obtained from blends of PS-CdS and PS-*b*-PEO2 deposited from chloroform solutions of 2.0 mg/mL for various weight fractions of PS-CdS within the blend ( $f$ ). For relatively low PS-CdS content in the blend (Figure 3a;  $f = 0.25$ ), nanowire-like assemblies are observed; although, unlike the structures in Figure 2, the width along the length of these wires is not uniform, and nodules periodically spaced along the nanowires are clearly visible. The mean height and width of the nodules ( $h = 26 \pm 4$  nm and  $w = 310 \pm 60$  nm) are both greater than the narrower parts of the wires ( $h = 15 \pm 2$  nm and  $w = 180 \pm 30$  nm), which have dimensions similar to the spaghetti structures formed from PS-*b*-PEO2 alone; TEM images of these structures confirmed that CdS NPs are localized within the nodules. As the PS-CdS content increases, the height and width along the length of the assemblies becomes more uniform, with the nanowire dimensions at  $f = 0.75$  being similar to those of the nodules formed at  $f = 0.25$  (Figure 3c;  $h = 27 \pm 3$  nm and  $w = 320 \pm 30$  nm); TEM images showed NPs evenly distributed along the length of these more uniform 1D structures.

Figure 3c also highlights an additional interesting surface feature: NP/polymer nanowires with nanoring connectors, which was a prominent morphology for  $f = 0.75$  but was rarely observed at other compositions. Along with the transition from nodules to more uniform 1D assemblies, NP/polymer surface features were generally found to be longer, with less branching, as the PS–CdS content increased. Similar trends were observed for blends of PS–CdS with the more hydrophobic PS-*b*-PEO1. We note that the heights of both the nodules and the nanowires formed from blends of PS–CdS and PS-*b*-PEO2 (~26 nm) suggest a monolayer of PS–CdS stabilized at the air–water interface by the PS-*b*-PEO brush structure (Scheme 1), similar to the structures in Figure 2 formed from the PS-*b*-PEO1-containing blends; however, the composite features containing PS-*b*-PEO2 are slightly taller than those containing PS-*b*-PEO1 (~21 nm), which is consistent with the somewhat longer PS block within the brush. For the same blend concentration and PS–CdS content, the widths of the nanowires and nanocables formed using the two PS-*b*-PEO copolymers were very similar; for example, for 2.0 mg/mL blend solutions with  $f = 0.75$ , 1D features containing PS-*b*-PEO1 and PS-*b*-PEO2 had mean widths of  $w = 320 \pm 40$  and  $w = 320 \pm 30$ , respectively. A more complete description of the effects of blend composition and concentration for blends of PS–CdS with both of the PS-*b*-PEO copolymers will be presented in an upcoming full publication.

The glassy PS matrix of the surface features gives rise to excellent mechanical resilience, and the observed morphologies were stable to changes in the LB surface pressure and to repeated compression–expansion cycles. In the TEM image in Figure 3d, a tear has developed in the Formvar substrate, which exerts a tensile stress on a nanowire that has been heated by the electron beam; interestingly, the nanowire undergoes extension without rupture, a property attributable to the viscoelastic nature of the heated PS matrix.

In conclusion, this strategy of synergistic self-assembly at the air–water interface offers new routes to NP/polymer assemblies with potential photonics applications because the nanoscale organization of NPs is coupled to length scales that are commensurate with optical wavelengths. The mechanical resilience of these assemblies and the ability to control aggregate densities on various substrates by LB transfer should allow individual hybrid features to be isolated for study as potential elements in photonic devices; for example, polymeric nanocables, branched nanowires, and nanowires with nanoring connectors, all containing densely packed photoluminescent NPs, could serve as “active waveguides”<sup>23</sup> of different geometries in photonic circuits. Additionally, LB transfer has been shown to induce the preferential orientation of nanowires, with the potential for forming ordered arrays of surface features from more uniform populations of aggregates. Achieving further control over the morphologies and dimensions of these unique hybrid surface features and understanding the mechanism of synergistic interfacial self-assembly are topics of current investigation in our group.

**Acknowledgment.** The authors gratefully acknowledge the National Science and Engineering Research Council (NSERC), the Canadian Foundation for Innovation (CFI), and the British Columbia Knowledge Development Fund (BCKDF) for their generous support of the research.

**Supporting Information Available:** Experimental details on the preparation and characterization of the NP/polymer hybrid assemblies is provided in Supporting Information. This material is available free of charge via the Internet at <http://pubs.acs.org>.

LA0519397

(23) Barrelet, C. J.; Greytak, A. B.; Lieber, C. M. *Nano Lett.* **2004**, *4*, 1981.